Jouini, H.; Martinez-Ortigosa, J.; Mejri, I.; Mhamdi, M.; Blasco Lanzuela, T.; Delahay, G. (2019). On the performance of Fe-Cu-ZSM-5 catalyst for the selective catalytic reduction of NO with NH3: the influence of preparation method. Research on Chemical Intermediates. 45(3):1057-1072. https://doi.org/10.1007/s11164-018-3658-8

On the Performance of Fe-Cu-ZSM-5 catalyst for the Selective Catalytic Reduction of NO with NH_3: The Influence of Preparation Method

Houda Jouini [1] · Joaquin Martinez-Ortigosa [2] · Imène Mejri [3,4] · Mourad Mhamdi [3, 4] · Teresa Blasco [2] · Gérard Delahay [5]

[1] Université de Tunis El Manar, Faculté des Sciences de Tunis, LR01ES08 Laboratoire de Chimie des Matériaux et Catalyse, 2092, Tunis, Tunisie.
[2] Instituto de Tecnología Química, Universitat Politècnica de València - Consejo Superior de Investigaciones Científicas (UPV-CSIC), Avda. de los Naranjos s/n, 46022 Valencia, Spain.
[3] Université de Tunis El Manar, Institut supérieur des technologies médicales de Tunis, 1006, Tunis, Tunisie.
[4] Ecole Nationale Supérieure de Chimie de Montpellier, Equipe MACS (site La Galera), 240 avenue du Professeur Emile Jeanbrau, CS 60297 34296 Montpellier, Cedex 05, France.

Houda Jouini
+216 99 92 56 55
houda.jouini@fst.utm.tn

Abstract The Selective Catalytic reduction of NO with ammonia (NH_3-SCR) in the presence of H_2O was studied over a series of Fe-Cu-ZSM-5 catalysts prepared by solid-state ion exchange (SSIE), aqueous ion exchange and dry impregnation methods. The prepared samples were characterized by a wide number of techniques (ICP-AES, N_2 physisorption at 77 K, XRD, STEM-EDX, XPS, H_2-TPR and DRS UV-vis) to investigate the effect of the preparation method on the activity, texture, structure and metal speciation of the studied catalysts. It was found that the aqueous ion exchange method induced a significant metal loss during the preparation procedure but without any activity deterioratation of the catalyst which encloses highly dispersed metal species. The catalysts prepared by SSIE and impregnation showed the highest metal contents and a large number of oxide aggregates leading to an activity decline at high reaction temperatures due to the ammonia oxidation phenomenon.

Keywords Ion exchange · Impregnation · NO · NH_3-SCR · Zeolite

Introduction

Fe-Cu-ZSM-5 system has been under intense investigation during the last five years for its exceptionally high activity for the decomposition of NO to N_2 during the SCR process [1-3]. This observation has stimulated many studies aiming to identify the nature of the active species involved in the SCR mechanism. Various methods for Fe-Cu-ZSM-5 preparation were described in the literature including excess-solution impregnation [4], improved incipient-wetness impregnation [2], subsequent aqueous ion-exchange1, solid-state ion exchange [3], and chemical vapour deposition [5]. However, the comparison of effectiveness of these methods was not very documented. Kröcher et al. [5] reported that the initial activity of the solid Fe-Cu-ZSM-5 was not influenced by the exchange method, but with regard to the stability of the catalyst, the exchange of vapour phase ions has been clearly favoured. However, in order to facilitate the preparation of the catalyst, liquid phase ion exchange and solid-state ion exchange are the preferred methods. T. Zhang attributed the high NH_3-SCR activity of Fe(4%wt)-Cu(4%wt)-ZSM-5 to the presence of highly dispersed Fe-Cu nanocomposites [2]. The interaction between Fe and Cu species in the Fe-Cu nanocomposites leads to the increase of the catalyst redox ability and the creation of additional acid sites on its surface compared to Cu (4%wt)-ZSM-5 catalyst. Sultana et al. have shown that the performances of Fe-Cu-ZSM-5 catalysts prepared by aqueous ion exchange and solid ion exchange are similar [3]. Both methods of preparation led to dispersed metal ions and a considerable amount of iron oxide. The present study was undertaken with the aim of optimizing the most appropriate method for the preparation of Fe-Cu-ZSM-5 catalyst.

Experimental

Catalysts preparation

Three preparation methods were adopted for the preparation of Fe(2%wt)-Cu(1.5%wt)-ZSM-5 catalysts: aqueous ion exchange, dry impregnation and solid-state ion exchange. Iron and

copper precursors were provided by Sigma-Aldrich. The commercial NH_4^+-ZSM-5 (CBV024E, Si/Al=15) zeolite was supplied by Zeolyst International.

Sample 1: it was prepared by the aqueous ion exchange method by mixing under reflux (80 °C, 48 h) 1 g of zeolite with 50 mL of aqueous copper chloride solution containing the desired amount of the $CuCl_2.2H_2O$ precursor. The mixture was then centrifuged and washed with distilled water. The collected product is dried for 24 hours at 110 °C and then treated at 400 °C (2 °C min^{-1}) for 1h under a stream of helium (99.99%, Air Liquide, 30 cm^3 min-1). The obtained solid was then exchanged with 50 mL of an aqueous solution of iron chloride ($FeCl_2 \cdot 6H_2O$) and the previous procedure was repeated following the same steps.

Samples 2 and 3: they were prepared by one-step aqueous ion exchange and were considered as reference materials. Sample 2 was issued from $CuCl_2.2H_2O$ only while sample 3 was issued from $FeCl_2.6H_2O$ only.

Sample 4: it was prepared by the dry impregnation method. 1 g of zeolite was mixed in a rotary evaporator (80 °C, 4h) with the desired amount of $CuCl_2.2H_2O$ dissolved in a minimum of water. The resulting mixture was dried at 110 °C for 12 h. This procedure was repeated by mixing the dried solid with the desired amount of iron chloride ($FeCl_2 \cdot 6H_2O$) dissolved in a minimum of water. The obtained sample was calcined at 550 °C (2 °C min^{-1}) for 8 h in air stream.

Sample 5: it was prepared by the solid-state ion exchange method: 1 g of zeolite was mixed and finely ground with the desired amount of $CuCl_2.2H_2O$ in an agate mortar for 5 min under ambient conditions. The resulting mixture was then heated under a stream of helium (99.99%, Air Liquide, 30 cm^3 min^{-1}) for 12 h at 380 °C (2 °C min^{-1}). The obtained powder was mixed and finely ground with the desired amount of $FeCl_2 \cdot 6H_2O$, then heated for 12 h at 290 °C in a stream of helium and under the same conditions described previously.

The prepared catalysts were labeled Fe-Cu-Z-AQ, Cu-Z-AQ, Fe-Z-AQ, Fe-Cu-Z-IM and Fe-Cu-Z-SS, where Z represents the parent zeolite ZSM-5 and the terms AQ, IM and SS denote the aqueous exchange, impregnation and solid-state ion exchange, respectively.

Activity measurements

The NH_3-SCR of NO catalytic test was performed in temperature programmed surface reaction (TPSR) using a flow reactor operating at atmospheric pressure with a space velocity of 333.333 h^{-1} and a total flow rate of 6 L h^{-1}. The concentrations of NH_3 and NO were established from initial gas cylinders containing 0.75% of NH_3 and 0.75% of NO in helium respectively. 18 mg of each sample were activated in-situ at 250 °C under oxygen and helium mixture (8% O_2/He) and then cooled to 200 °C. After reaching the starting reaction temperature, a by-pass of the reactor is done. From this step, the gas outlet composition was continuously monitored by vacuum stripping a fraction of the exit gas with a capillary towards the mass spectrometer (Pfeiffer Omnistar) equipped with Channeltron and Faraday detectors (0-200 amu) following the characteristic masses of : NH_3 (m/z =15, NH^+), H_2O (m/z =18, H_2O^+), N_2 (m/z = 28, N_2^+), NO (m/z = 30, NO^+), N_2O (m/z = 44, N_2O^+). Firstly, baselines of NH_3 (m/z =15, NH^+), N_2 (m/z = 28, N_2^+), NO (m/z = 30, NO^+) and N_2O (m/z = 44, N_2O^+) were done under the mixture containing He, O_2 and water only (3.5% H_2O, 8% O_2 and 88.5% He). Then, the adequate flowrates of 0.75% NO/He and of 0.75% of NH_3/He were introduced and the He flowrate adjusted in order to obtain the following gas composition: 1000 ppm of NO and 1000 ppm of NH_3. After attaining the stability of all characteristic mass lines, NO and NH_3 are introduced (mass flowmeters) and by adjusting the He flow, the reaction mixture is ready. Then, the by-pass is removed and the reaction mixture starts to pass through the catalyst. After 10 minutes of dwell, the temperature was increased from 200 °C to 550 °C. The catalytic results were expressed as follows:

Conversion of the reactant R (R=NO or NH_3):

$X_R = \frac{[R_0]-[R_T]}{[R_0]} \times 100$, where $[R_0]$ and $[R_T]$ are the concentrations of the reactant R at the inlet gas reactor and at the temperature T, respectively.

Amount of N_2O formed:

$Q_{N_2O} = \frac{[N_2O_T]-[N_2O_{inj}]}{[N_2O_0]-[N_2O_{inj}]} \times 1000$, where $[N_2O_{inj}]$ is the concentration of N_2O before injection, $[N_2O_T]$ and $[N_2O_0]$ represent the concentrations of N_2O at athe temperature T and at the inlet gas reactor, respectively.

Selectivity toward N_2:

$$S_{N_2} = \frac{\left[(X_{NO} \times 1000) + (X_{NH_3} \times 1000)\right] - Q_{N_2O}}{(X_{NO} \times 1000) + (X_{NH_3} \times 1000)} \times 100$$

Catalyst characterization

The chemical analysis of the studied materials was carried out by ICP-AES in a Varian 715-ES. The powder samples (ca 20-30 mg) were dissolved in an acid mixture of 20%HNO3:20%HF: 60%HCl (% vol) and aged during 24h. In all cases, the calibration curve was fitted to the predicted approximate concentration of analyte and determined using standard solutions (Sigma-Aldrich). The wavelengths used for Cu and Fe analysis were 327.395 and 234.350 nm, respectively. The samples crystallinity was checked using a PANanlytical Cubix'Pro diffractometer equipped with an X'Celerator detector and automatic divergence and reception slits using Cu-Kα radiation (0.154056 nm). The equipment is working under a voltage of 45 kV and a current of 40 mA. The diffractograms were recorded in the region of 5-40 ° and were exploited with the software PANalytical X'Pert HighScore Plus. The phase identification was accomplished by comparing the experimental

diffractograms with the references of the international database ICDD (The International Centre for Diffraction Data). STEM observations were performed using a JEOL-JEM 2100F instrument equipped with an X-MAX microanalysis detector and operating under an accelerating voltage of 200 kV and a resolution energy of 20 eV. N_2 physisorption measurements were determined with an automatic ASAP 2020 apparatus from Micromeritics. Before the nitrogen adsorption, the samples were outgassed at 250 °C until a static vacuum of 3×10^{-5} bar was reached. BET model was used to calculate the specific surface area, while pore volumes were calculated at the end of the step corresponding to the filling of the pores (at P/P°=0.98). The samples crystallinity was checked using a PANanlytical Cubix'Pro diffractometer equipped with an X'Celerator detector and automatic divergence and reception slits using Cu-Kα radiation (0.154056 nm). The equipment is working under a voltage of 45 kV and a current of 40 mA. The diffractograms were recorded in the region of 5-40° and were exploited with the software PANalytical X'Pert HighScore Plus. The phase identification was accomplished by comparing the experimental diffractograms with the references of the international database ICDD (The International Centre for Diffraction Data). STEM observations were performed using a JEOL-JEM 2100F instrument equipped with an X-MAX microanalysis detector and operating under an accelerating voltage of 200 kV and a resolution energy of 20 eV. DRS UV-vis measurements were performed on a Perkin Elmer Lambda 45 spectrophotometer equipped with a diffuse reflectance attachment. Spectra were recorded at room temperature in the wavelength range of 200-900 nm using BaSO4 as reference material. H_2-TPR profiles were obtained on an automated Micromeritics Autochem 2920 analyser. Before H_2-TPR measurements, samples (50 mg) were pre-treated in a quartz U-tube reactor under 5%O_2/He flow (30 cm^3 min^{-1}) at 500 °C (10 °C min^{-1}) for 30 min and then cooled under helium to 40 °C. The samples were then reduced from 40 to 800 °C (5 °C min^{-1}) under 5%H_2/Ar atmosphere (30 cm^3 min^{-1}). XPS analyzes were performed using a SPECS

spectrometer equipped with a MCD-9 detector. The source is composed of an aluminum anode emitting monochromatic X-ray radiation (Kα = 1486.6 eV).

Results

NH_3-SCR catalytic activity

The prepared catalysts were tested in the SCR of NO with ammonia and the collected results were shown in Fig.1. Table 1 summarizes the reaction temperatures of tested catalysts corresponding to 50% (T_{50}) and 100% (T_{100}) of conversion and the operating temperature window (temperature range for which the NO conversion is of 100%).

Fig.1 NO conversion over Fe-Cu-Z-AQ, Fe-Cu-Z-IM and Fe-Cu-Z-SS catalysts. Feed: 1000 ppm NO, 1000 ppm NH_3, 3.5% H_2O, 8% O_2 and 88.3% He. Flowrate: 6 L h^{-1}. Space velocity: 333.333 h^{-1}. Catalyst: 18 mg.

An examination of Fig. 1 and Table 1 shows that the Fe-Cu-Z-AQ catalyst exhibits the lowest conversion at the beginning of the reaction, which slowly increases to 50% at around 280 °C and 100% at about 409 °C. The conversion of NO remains lower than that of the Fe-Cu-Z-IM and Fe-Cu-Z-SS solids up to around 480 °C, where the activities of the latter decrease rapidly because of the ammonia oxidation phenomenon. The conversion of Fe-Cu-Z-AQ is kept around 100% at a higher temperature and this catalyst will have the widest SCR window. The catalysts Fe-Cu-Z-IM and Fe-Cu-Z-SS have the same catalytic profile up to 262 °C, beyond this temperature, the solid resulting from the impregnation method showed the best performance catalytic and reaches 50% and 100% conversion at lower temperatures than other catalysts. Beyond 310 °C, the Fe-Cu-Z-SS catalyst exhibited the same behavior as Fe-Cu-Z-AQ up to 484 °C when the ammonia oxidation phenomenon began to occur. This solid presented the narrowest SCR window and was the most delayed in reaching its maximum conversion (417 °C).

Table 1 NH_3-SCR of NO operating temperatures.

N_2 selectivity was above 90% over all the catalysts as shown in Fig. 2. The yield of N_2 in the presence of Fe-Cu-Z-AQ was the most important over the entire temperature range.

Fig. 2 N_2 selectivity over Fe-Cu-Z-AQ, Fe-Cu-Z-IM and Fe-Cu-Z-SS catalysts.

ICP-AES chemical analysis and N_2 physisorption at 77 K results

The chemical analysis was carried out by ICP-AES technique, Table 2 gathers the contents of iron and copper expressed in %wt as well as the percentages of metal loss. Examination of these results shows that iron and copper were well retained by the zeolite during the solid-state ion exchange and impregnation processes where the experimental values are in perfect agreement with the theoretical amounts set for the catalysts preparation. This result is expected since SSIE and impregnation methods are the most practical for introducing precise metal amounts into the zeolite. The ICP analysis also shows a significant loss of iron (32%) and copper (73%) in the case of Fe-Cu-Z-AQ. In fact, during the aqueous ion exchange procedure, the formed metal species, rather voluminous due to the solvation phenomenon, are hardly diffused to the exchange sites of the ZSM-5 which is characterized by small pore system. ICP-AES results (Table below) showed that the subsequent Fe-exchange eliminates an amount of copper, although the presence of copper improves the iron exchange

Table 2 Results of ICP-AES and N_2 physisorption at 77 K.

The textural properties of the prepared samples did not deteriorate from those of ZSM-5 as revealed the N_2 physisorption at 77 K analysis, indicating that the texture of the parent zeolite was maintained after the various preparation processes. The decrease of textural properties in the case Fe-Cu-Z-IM and Fe-Cu-Z-SS was quite important. This result can be explained by the possible presence of Fe and/or Cu oxide agglomerates which may partially

block the pores or the channels of the zeolite thus limiting the accessibility of the nitrogen. Examination of Table 2 shows that the zeolite S_{BET}, the pore volume and size undergo a slight decrease after the introduction of Fe and Cu by aqueous ion exchange dismissing the possibly of pore blocking by large oxide species and suggesting their incorporation in the exchange sites of the zeolite.

XRD and STEM results

The STEM image of the Fe-Cu-Z-AQ (Fig. 3a) does not reveal the presence of any oxide particles in the different observed areas. In this sample, copper species were highly dispersed, while iron species were more agglomerated, as shown in the EDX mapping image. In the case of Fe-Cu-Z-IM (Fig. 3b), large Cu oxide particles of size between 4 and 18 nm (spectra 52 and 54) and smaller Fe particles (spectrum 53) with a size not exceeding 5 nm were both observed. The size of these particles leads us to speculate that they are located on the zeolite outer surface [6]. The STEM image of Fe-Cu-Z-SS (Fig. 3c) reveals the presence of iron particles (spectrum 25) of size up to 8 nm; they coexist with Fe-Cu nanocomposites (spectrum 22) with an average size of 5 nm.

Fig. 3 STEM micrographs and EDX elemental mapping of fresh (a) Fe-Cu-Z-AQ, (b) Fe-Cu-Z-IM et (c) Fe-Cu-Z-SS. Accelerating voltage: 200 kV. Resolution energy: 20 eV.

Fig.4 shows the XRD diffractograms of the parent zeolite and the Fe-Cu-Z solids. All the samples show the typical diffractions of the MFI structure, evidencing the stability of the zeolite structure after the different preparation processes.

Fig. 4 XRD patterns of fresh NH_4^+-ZSM-5, Fe-Cu-Z-AQ, Fe-Cu-Z-IM and Fe-Cu-Z-SS. Radiation: Cu-Kα (0.154056 nm). Voltage : 45 kV. Current : 40 mA.

The correspondence of the recorded diffractograms with the ICDD PDF reference models by the "peak matching" method revealed the presence of Fe_2O_3 (ICDD PDF#33-0664), CuO (ICDD PDF#48-1548) and Fe_2CuO_4 (ICDD PDF#33-0664) phases over Fe-Cu-Z-IM and Fe-Cu-Z-SS although oxide peaks were not detected in the samples diffractograms. This is due to the low metal amount introduced in the zeolites (around 1%wt) which is in the limit of detection of the XRD equipment, besides the metals fluorescence (especially Fe) which considerably decreases the peaks intensity of the oxide particles. The small size of oxide nanoparticles provides broad XRD peaks, which overlap with those of MFI zeolite.

XPS results

Fig. 5b shows the Fe 2p spectrum, the characteristic peak of Fe $2p_{3/2}$ was detected for the three studied samples at about 711 eV. Its deconvolution led to two distinct bands centered at 710.9 and 713.8 eV and assigned to Fe $2p_{3/2}$ binding energies of FeO and Fe_2O_3 species, respectively, indicating that iron is present in the form of Fe^{2+} and Fe^{3+} [7]. The Cu $2p_{3/2}$ spectrum (Fig. 5a) was also detected for all the studied catalysts, it was decomposed into two bands around 931-932 eV and 933-934 eV, assigned to Cu^{+} and Cu^{2+} species respectively [8]. The relative concentration of Cu and Fe ions as well as Cu^{+}/Cu^{2+} and Fe^{2+}/Fe^{3+} ratios are shown in Table 3. We can notice that the surface of Fe-Cu-Z catalyst is mainly covered by divalent Fe and Cu species. With reference to the works of J. Zhang et al. [9], the redox mechanism of the NH_3-SCR reaction consists of electron transfer processes between the Cu^{n+} and Fe^{n+} ions. The presence of the $Fe^{3+/}Fe^{2+}$ and $Cu^{2+/}Cu^{+}$ redox couples promotes the formation of oxygen vacancies at the catalyst surface that help in accelerating the NO to NO_2 oxidation process, known as the critical step in the SCR process [10].

Fig.4 Cu 2p (a), (b) Fe 2p and (c) O 1s XPS spectra of fresh Fe-Cu-Z-AQ. Source: aluminum anode. Radiation: Kα = 1486.6 eV.

The signal O1s, presented in Fig. 5c, was decomposed into three bands corresponding to different species: framework oxygen of the Fe/Cu-O bonds, the oxygen of the framework oxygen of Si-O bonds and chemisorbed oxygen (band centered on 532 eV), known as one of the most active oxygen species [10]. The examination of Table 3 reveals that the sample Fe-Cu-Z-IM contains the largest amount of chemisorbed oxygen (14.88%) and the highest Cu^{+}/Cu^{2+} and Fe^{2+}/Fe^{3+} proportions. The increase of these proportions results in the increase of the chemisorbed oxygen content: the redox couples promote the formation of oxygen vacancies, which are advantageous for the adsorption of oxygen on the surface of the catalyst leading to the formation of chemisorbed oxygen species [11].

Table 3 XPS quantitative analysis.

H_2-TPR results

The H_2-TPR profile of the sample Fe-Cu-Z-AQ is presented in Fig. 6a, it has been deconvolved into four gaussians centred at 358, 434, 562 and 691 °C whose assignment is explained as follows: the peak at T <400 ° C corresponds to the reduction of Cu^{+} species to Cu^{0} and/or Fe^{3+} to Fe^{2+} [12], the one centred at 434 °C corresponds to the reduction of Fe (III)-oxo ions in the cationic positions or that of the nanometric Fe_3O_4 clusters in FeO [1] and the two peaks at T> 500 °C are attributed to the reduction of Fe^{2+} species to Fe^{0} [5]. The peak at 691 °C was attributed by another group of researchers to the two-step Fe_2O_3 reduction as the sequence: $Fe_2O_3 \rightarrow Fe_3O_4 \rightarrow Fe^{0}$ [13].

Fig. 6 H_2-TPR profiles of (a) Fe-Cu-Z-AQ, (b) Fe-Cu-Z-IM and (c) Fe-Cu-Z-SS. Pre-treatment: 30 min at 500 °C (10 °C min^{-1}) under 5%O_2/He flow (30 cm^3 min^{-1}) and then cooled under helium to 40 °C. Sample: 50 mg.

The TPR profile of Fe-Cu-Z-IM (Fig. 6b) shows a peak at 358 °C attributable to the reduction of Cu^{+} to Cu^{0} and/or Fe^{3+} to Fe^{2+}. The corresponding hydrogen consumption is greater than that observed with Fe-Cu-Z-AQ at the same reduction temperature, which could be due to a

larger content of Fe(III) and/or Cu(I). The two peaks at 414 and 482 °C can be attributed to the reduction of Fe^{3+} and/or Fe_3O_4 species to Fe^{2+}, while the two peaks centred at 574 °C and 621 °C result from the reduction of Fe^{2+} to Fe^0 [2].

The profile of Fe-Cu-Z-SS (Fig. 6c) can be decomposed into four reduction zones: Cu^{2+} to Cu^+ at T <300 ° C [2,1], Cu^+ to Cu^0 and/or Fe^{3+} to Fe^{2+} at 300 °C <T <400 °C, Fe^{3+} and/or Fe_3O_4 to Fe^{2+} at 400 °C <T <500 °C and Fe^{2+} to Fe^0 at T> 500 °C.

The obtained H_2-TPR results show that the copper species are reduced at lower temperatures in the case of catalysts prepared by impregnation and solid-state exchange compared to that prepared by aqueous exchange. In fact, the easier the reduction of these species is, the higher their redox capacity is in the reaction studied. The presence of such easily reducible species oxidizes NO to NO_2 and nitrates, which are intermediate species controlling the rate of SCR reaction and NO conversion at low temperatures [1]. However, such Cu species lead to low NO conversion at elevated temperatures due to their activity in the competing NH_3 oxidation reaction.

DRS UV-vis results

The valence and coordination state of Fe and Cu species present in the prepared catalysts were determined by UV-vis spectroscopy. The Kubelka-Munk function was calculated from reflectance measurements and the recorded spectra are shown in Fig. 7.

Fig. 7 DRS UV-vis spectra of fresh (a) Fe-Cu-Z-AQ, (b) Fe-Cu-Z-IM and (c) Fe-Cu-Z-SS. Temperature: room temperature. Reference material: $BaSO_4$.

Examination of the UV-vis spectrum of Fe-Cu-Z-AQ (Fig. 7a) shows the fundamental absorption bands of the zeolite matrix at 211 and 272 nm [14]. The second band can also be attributed to isolated Fe^{3+} species in pseudo-tetrahedral coordination [15]. The spectrum of

Fe-Cu-Z-SS (Fig. 7c) exhibits two absorption bands at 227 and 254 nm: the first is a d-d charge transfer band assigned to Fe^{3+} species in tetrahedral coordination ($e \rightarrow t_2$) [16], while the second comes mainly from the p-d charge transfer transition between the framework oxygen and Fe^{3+} cations [17]. Another band appearing at 356 nm has been assigned to oligonuclear $Fe^{3+}xOy$ clusters [18]. In addition to the basic absorption band of the zeolite matrix at 207 nm, the UV-vis spectrum of Fe-Cu-Z-IM (Fig. 7b) shows the p-d charge transfer band of isolated Fe^{3+} ions at 256 nm. Moreover, two broad bands located at $\lambda > 600$ nm attributable to $t_{2g} \rightarrow e_g$ transitions of Cu^{2+} ions in octahedral symmetry are observed for both Fe-Cu-Z-AQ and Fe-Cu-Z-IM samples [19].

Discussion

The selective catalytic reduction of NO was studied over a series of Fe-Cu-ZSM-5 catalysts prepared by three different methods. Changes in the structure and texture of the parent zeolite after the different preparation processes were investigated using XRD and N_2 physisoption at 77 K techniques. The comparison between the XRD diffractogram of ZSM-5 and those of the prepared solids suggests that the parent zeolite structure has not been modified and that its crystallinity remains intact. The texture of ZSM-5 was also maintained. Fe-Cu-Z-AQ exhibits the most important specific surface area: a large S_{BET} helps to better disperse the metal species. This result is in perfect agreement with STEM observations showing the lowest degree of metal aggregation for Fe-Cu-Z-AQ. The pore volume of this solid has not been modified; suggesting the absence of oxide particles that may block the entry of the zeolite pores and inhibits the accessibility of nitrogen. Again, the STEM technique confirms this hypothesis since no oxide particle was detected in the case of Fe-Cu-Z-AQ. The absence of such particles may explain the absence of the ammonia oxidation phenomenon in the case of this catalyst. Chemical analysis by ICP shows that Fe-Cu-Z-AQ was the site of a significant metal loss during the different stages of the aqueous ion exchange process. This loss can

occur at three levels: (1) the metal species formed in solution, generally in the form of $[Fe(H_2O)_6]^{3+}$ and $[Cu(H_2O)_4]^{2+}$, are voluminous due to the phenomenon of solvation and are hardly diffused to the exchange sites of the ZSM-5 which is characterized by a small pore system (ring sizes: 5.1×5.5 Å and 5.3×5.6 Å). (2) An amount of non-exchanged metals can be lost during the washing step following the exchange procedure or (3) during the helium heat treatment, where some metal species weakly connected to the zeolite can volatilize. The weak Cu content (0.40%wt) of Fe-Cu-Z-AQ explains its low catalytic behavior at low temperature. This result is in agreement with the literature which assigns the low temperature activity to Cu species and mainly to isolated Cu^{2+} ions [20]. The ammonia oxidation did not occur in the case of this catalyst, such reaction is promoted by the presence of large metal oxide particles, mainly CuO [21]. Large CuO nanoparticles (18 nm) were observed in the STEM micrograph of Fe-Cu-Z-IM, which explains its activity towards the ammonia oxidation reaction. In the case of Fe-Cu-Z-SS, Cu oxide particles were not detected, only Fe_2CuO_4 nanocomposites of small sizes (5 nm) were present together with a limited number of Fe_2O_3 particles. These species are active during the ammonia oxidation process but remain less efficient than CuO species [22].

The decrease in textural properties is greater in the case of Fe-Cu-Z-IM and Fe-Cu-Z-SS samples. It is attribution to the partial occlusion of zeolite pores by iron and/or copper oxide agglomerates is possible since their existence is shown by STEM technique. The solid Fe-Cu-Z-SS exhibits the most significant decrease in the specific surface area and the average pore diameter; the observation of its surface by STEM microscopy reveals a fairly high degree of aggregation of both Fe and Cu species. It was noticed that the metal oxides formed in the case of Fe-Cu-Z-IM (Fe_2O_3 and CuO) and Fe-Cu-Z-SS (Fe_2O_3, Fe_2O_3 and Fe_2CuO_4) are of different nature. It has been reported that the heat treatment following the catalyst preparation procedure can influence the metal speciation [23]: calcination under air at moderate

temperatures (around 400 °C) leads to the formation of rich oxygen oxides, while less oxidized compounds are obtained when the heat treatment is carried out in an inert gas at higher temperatures (or during a longer treatment period as for Fe-Cu-Z-SS) which is in perfect agreement with our results.

XPS spectroscopy shows that the metal cations are present under oxidation states +I and +II for copper and +II and +III for iron, such species have also been demonstrated by UV-vis and H_2-TPR analyzes. The quantitative XPS study reveals that Fe-Cu-Z-IM exhibits the highest Cu^{+}/Cu^{2+} and Fe^{2+}/Fe^{3+} ratios (0.65 and 2.57, respectively) and also the highest percentage of chemisorbed oxygen. This catalyst showed the highest catalytic performance, a similar result was obtained in a previous study [8]: high Cu^{+}/Cu^{2+} and Fe^{2+}/Fe^{3+} ratios favor the adsorption of oxygen on the surface of the catalyst, forming chemisorbed oxygen species which are known to play an important role in the redox mechanism of the NH_3-SCR reaction [2,17]. Fe-Cu-Z-SS exhibits a higher Cu^{+}/Cu^{2+} ratio than Fe-Cu-Z-AQ and its low-temperature activity is found better. At high temperatures, Fe-Cu-Z-AQ becomes more active which can be correlated to its higher Fe^{2+}/Fe^{3+} ratio. The chemisorbed oxygen percentages of these two catalysts are similar, which explains their comparable catalytic performance.

Conclusion

According to many authors, the activity of ZSM-5 catalysts exchanged with transition metals depends on their preparation method [24-26]. The effect of the preparation method on the physicochemical and catalytic properties of the studied Fe-Cu-ZSM-5 catalyst was investigated in this study. The aqueous ion exchange method induced a significant metal loss during the various preparation steps although it did not deteriorate the catalytic activity of the issued catalyst which has been characterized by the best dispersion of Fe and Cu species and the absence of the ammonia oxidation phenomenon. The catalysts prepared by SSIE and

impregnation showed the highest metal contents but a different metal speciation and catalytic activity. The presence of oxide particles in these samples led to an activity decline at high reaction temperatures due to ammonia oxidation which was more significant in the case of Fe-Cu-Z-IM containing the largest oxide particles. On the basis of the coexistence of different oxidation states of the Cu and Fe for the studied catalysts, an interaction can occur between Cu and Fe species, leading to some electron transfer processes during the redox mechanism of NH_3-SCR. This process is responsible of the formation of a highly active oxygen species on the surface of the prepared catalysts.

Acknowledgments

Financial support by the MINECO of Spain through the Severo Ochoa (SEV-2016-0683) and CTQ2015-68951C3-1-R projects is gratefully acknowledged. The authors thank the Electron Microscopy Service of the Universitat Politècnica de València for STEM experiments. J. Martínez-Ortigosa (SEV-2012-0267-02) is grateful to Severo Ochoa Program for a predoctoral fellowship.

References

1. Sultana A, Sasaki M, Suzuki K, Hamada H (2013) Catal Commun 41: 21-25

2. Zhang T, Liu J, Wang D, Zhao Z, Wei Y, Cheng K, Jiang G, Duan A (2014) Appl Catal B Environ 148-149: 520-531

3. Jouini H, Mejri I, Martinez-Ortigosa J, Vidal-Moya A, Mhamdi M, Blasco T, Delahay G (2018) Microporous Mesoporous Mater 260:217-226

4. Nakhostin P, Panahi P, Salari D, Niaei A, Mousavi SM (2013) J Ind Eng Chem 19: 1793-1799

5. Brandenberger S, Kröcher O, Tissler A, Althoff R (2011) Ind Eng Chem Res 50: 4308-4319

6. Beznis NV, Weckhuysen BM, Bitter JH (2010) Catal Lett 138: 14-22

7. Roosendaal SJ, van Asselen BJ, Elsenaar W, Vredenberg AM, Habraken FHPM (1999) Surf Sci 442 : 329-337

8. Zhu L, Zhang L, Qu H, Zhong Q (2015) J Mol Catal A 409:207-215

9. Zhang J, Qu H (2015) Res Chem Intermed 41: 4961-4975

10. Zhang R, Zhong Q, Zhao W (2014) Appl Surf Sci 289: 237-244

11. Yang SX, Zhu WP, Jiang ZP (2006) Appl Surf Sci 252: 8499-8505

12. Boroń P, Chmielarz L, Dzwigaj S (2015) Appl Catal B Environ 168-169: 377-384

13. Ma L, Li J, Arandiyan H, Shi W, Liu C, Fu L (2012) Catal Today 184: 145-152

14. Ismagilov ZR, Yashnik SA, Anufrienko VF, Larina TV, Vasenin NT, Bulgakov NN, Vosel SV, Tsykoza LT (2004) Appl Surf Sci 226: 88-93

15. Marturano P, Drozdová L, Pirngruber GD, Kogelbauer A, Prins R (2001) Phys Chem Chem Phys 3: 5585-5595

16. Pérez-Ramírez J, Groen JC, Brückner A, Kumar MS, Bentrup U, Debbagh MN, Villaescusa LA (2005) J Catal 232: 318-334

17. Sun K, Fan F, Xia H, Feng Z, Li WX, Li C (2008) J Phys Chem C 112: 16036-16041

18. Bordiga S, Buzzoni R, Geobaldo F, Lamberti C, Giamello E, Zecchina A, Leofanti G, Petrini G, Tozzola G, Vlaic G (1996) J Catal 158: 486-501

19. Chanquía CM, Sapag K, Rodríguez-Castellón E, Herrero ER, Eimer GA (2010) Phys Chem Chem Phys 114: 1481-1490

20. Moreno-Gonzalez M, Hueso B, Boronat M, Blasco T, Corma A (2015) J Phys Chem Lett 6: 1011-1017

21. Sjövall H, Olsson L, Fridell E, Blint RJ (2006) Appl Catal B Environ 64: 180-188

22. Amores JMG, Escribano VS, Ramis G, Busca G (1997) Appl Catal B Environ 13: 45-58

23. Brandenberger S, Kröcher O, Tissler A, Althoff R (2008) Catal Rev Sci Eng 50: 4925-31

24. Krishna K, Seijger GBF, van den Bleek CM, Makkee M, Mul G, Calis HPA (2003) Catal Lett 86: 121-132

25. Joyner R, Stockenhuber M (1999) J Phys Chem B 103: 5963-5976

26. Hall WK, Feng XB, Dumesic J, Watwe R (1998) Catal Lett 52: 13-19

Table 2

NH_3-SCR of NO operating temperatures.

Catalyst	SCR window (°C) [a,b]	T_{50}(°C) [a]	T_{100}(°C) [a]
Fe-Cu-Z-AQ	131	280	409
Fe-Cu-Z-IM	106	265	391
Fe-Cu-Z-SS	67	270	417

[a] Temperature window corresponding to 100% of NO conversion expressed in °C, [b] Expressed in °C.

Table 2

Results of ICP-AES and N_2 physisorption at 77 K.

Sample	Fe (%wt)	Fe loss (%)	Cu (%wt)	Cu loss (%)	S_{BET} (m^2/g)	Pore volume (cm^3/g)	Pore size (Å)
NH_4^+-ZSM-5	-	-	-	-	362	0.22	118
Fe-Cu-Z-AQ	1.37	32	0.40	73	343	0.20	115
Cu-Z-AQ	-	-	0.90	40	259	0.12	72
Fe-Z-AQ	1.17	42	-	-	376	0.16	70
Fe-Cu-Z-IM	1.78	11	1.38	8	328	0.13	101
Fe-Cu-Z-SS	1.83	9	1.41	7	306	0.13	71

Table 3

XPS quantitative analysis.

Sample	O 1s	Fe 2p			Cu 2p		
	Chemisorbed O (%)*	Fe^{2+} (%)*	Fe^{3+} (%)*	Fe^{2+}/Fe^{3+}	Cu^+ (%)*	Cu^{2+} (%)*	Cu^+/Cu^{2+}
Fe-Cu-Z-AQ	12.80	69.43	30.57	2.27	22.96	77.04	0.29
Fe-Cu-Z-IM	14.88	72.01	27.99	2.57	39.37	60.63	0.65
Fe-Cu-Z-SS	12.91	67.18	32.82	2.04	33.79	66.21	0.51

* Atomic concentration of catalyst surface.

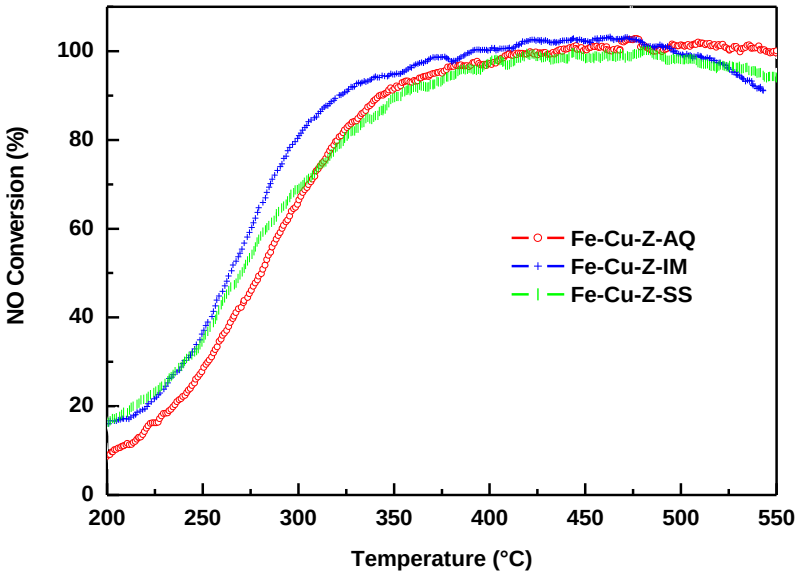

Fig.2 NO conversion over Fe-Cu-Z-AQ, Fe-Cu-Z-IM and Fe-Cu-Z-SS catalysts. Feed: 1000 ppm NO, 1000 ppm NH_3, 3.5% H_2O, 8% O_2 and 88.3% He. Flowrate: 6 L h^{-1}. Space velocity: 333.333 h^{-1}. Catalyst: 18 mg.

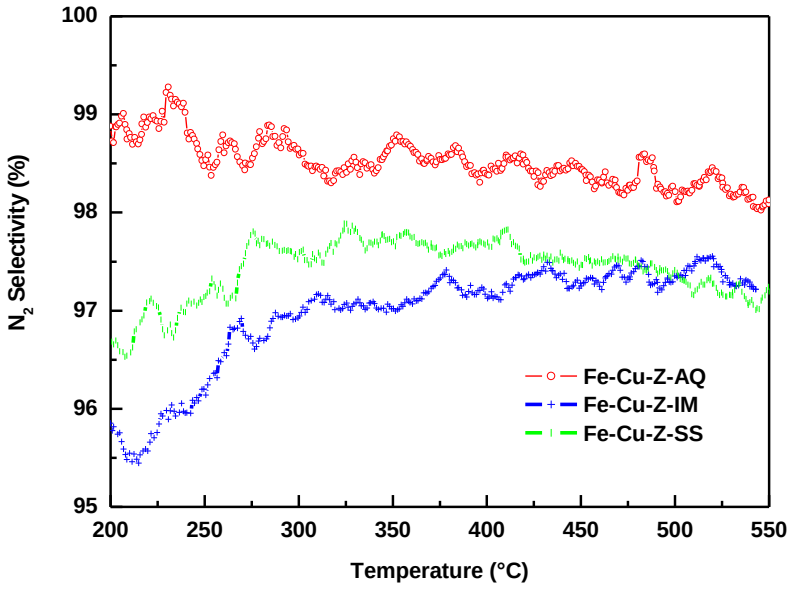

Fig. 2 N_2 selectivity over Fe-Cu-Z-AQ, Fe-Cu-Z-IM and Fe-Cu-Z-SS catalysts.

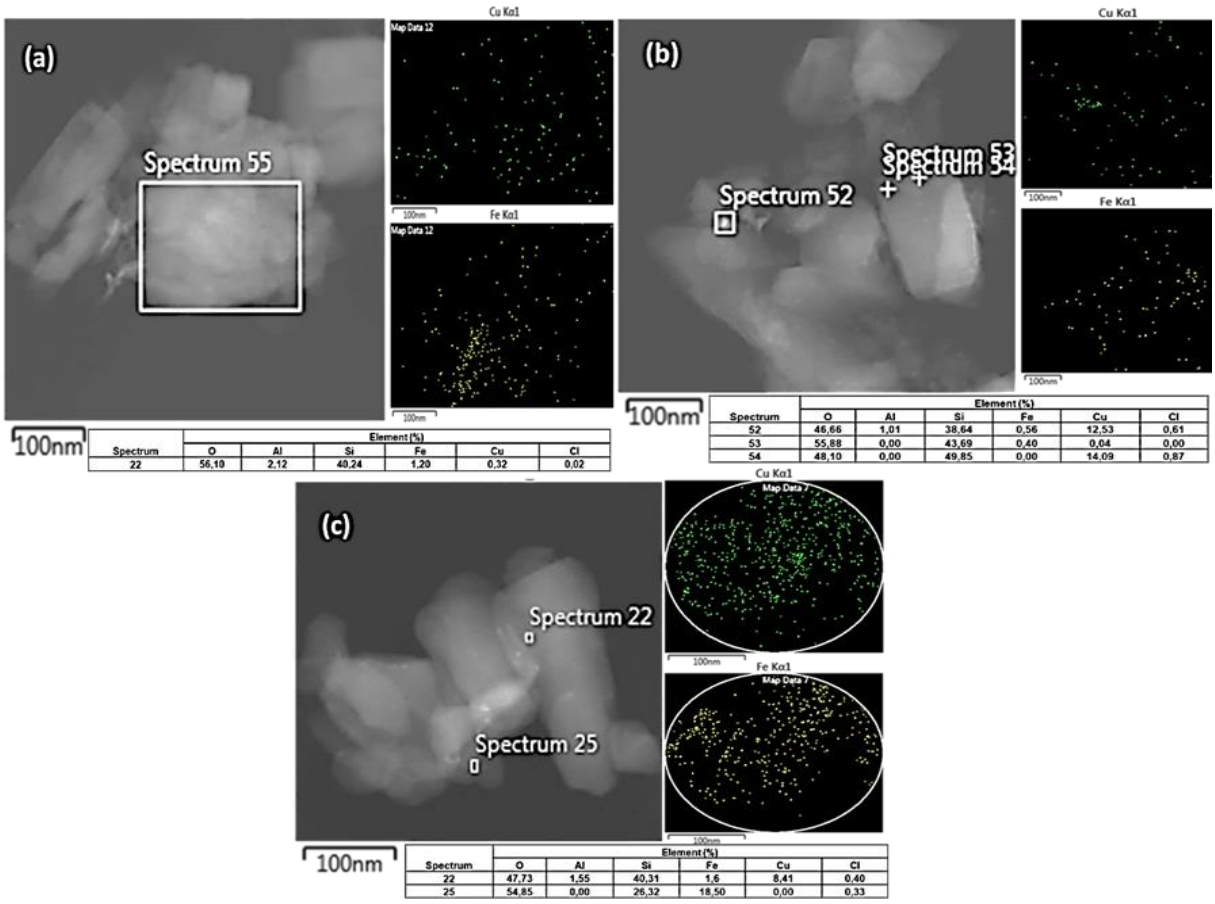

Fig. 3 STEM micrographs and EDX elemental mapping of fresh (a) Fe-Cu-Z-AQ, (b) Fe-Cu-Z-IM et (c) Fe-Cu-Z-SS. Accelerating voltage: 200 kV. Resolution energy: 20 eV.

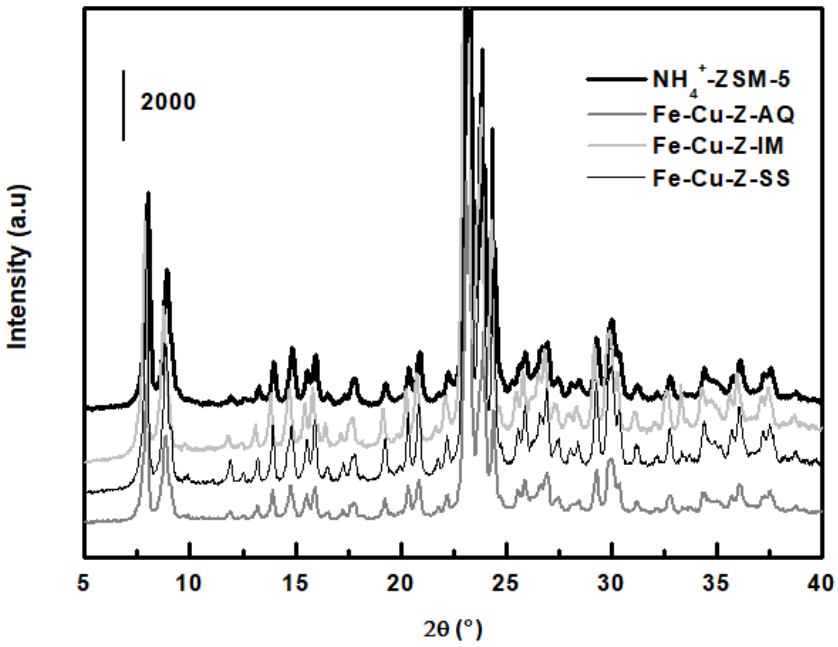

Fig. 4 XRD patterns of fresh NH_4^+-ZSM-5, Fe-Cu-Z-AQ, Fe-Cu-Z-IM and Fe-Cu-Z-SS. Radiation: Cu-Kα (0.154056 nm). Voltage: 45 kV. Current : 40 mA.

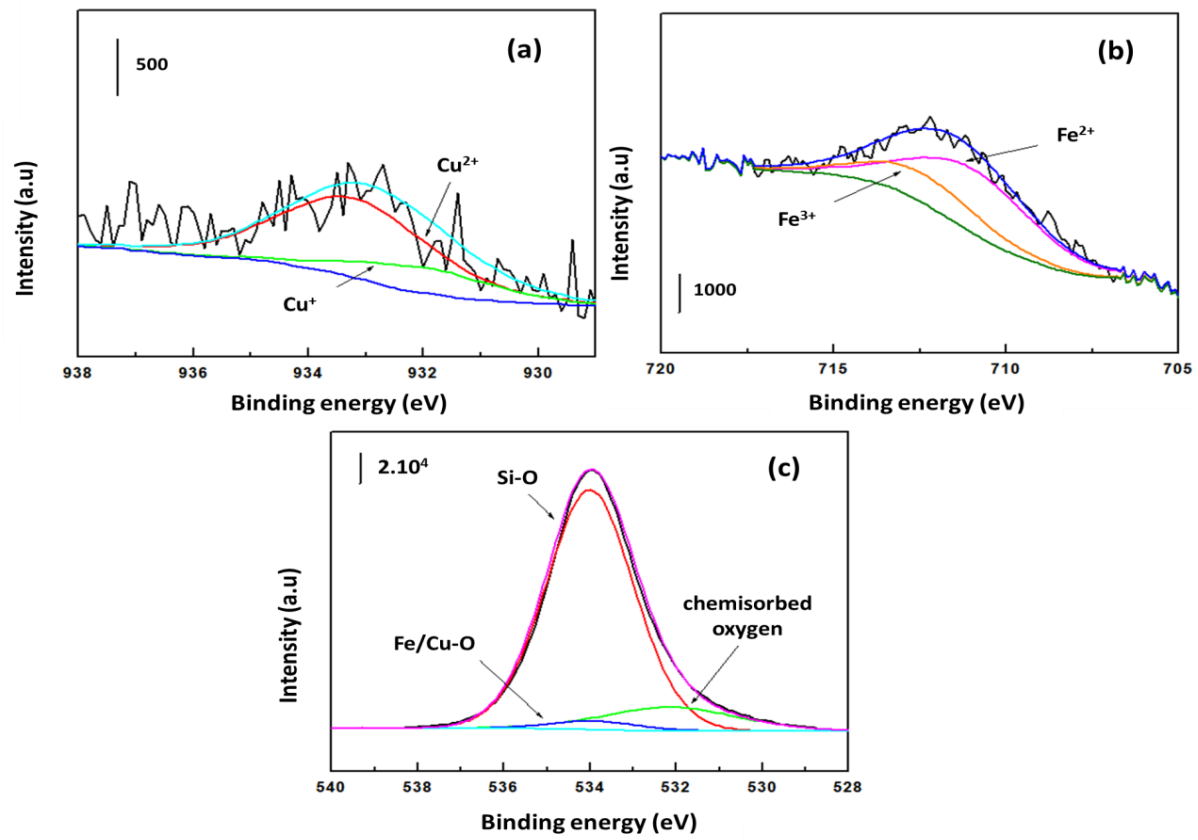

Fig. 5 Cu 2p (a), (b) Fe 2p and (c) O 1s XPS spectra of fresh Fe-Cu-Z-AQ. Source: aluminum anode. Radiation: Kα = 1486.6 eV.

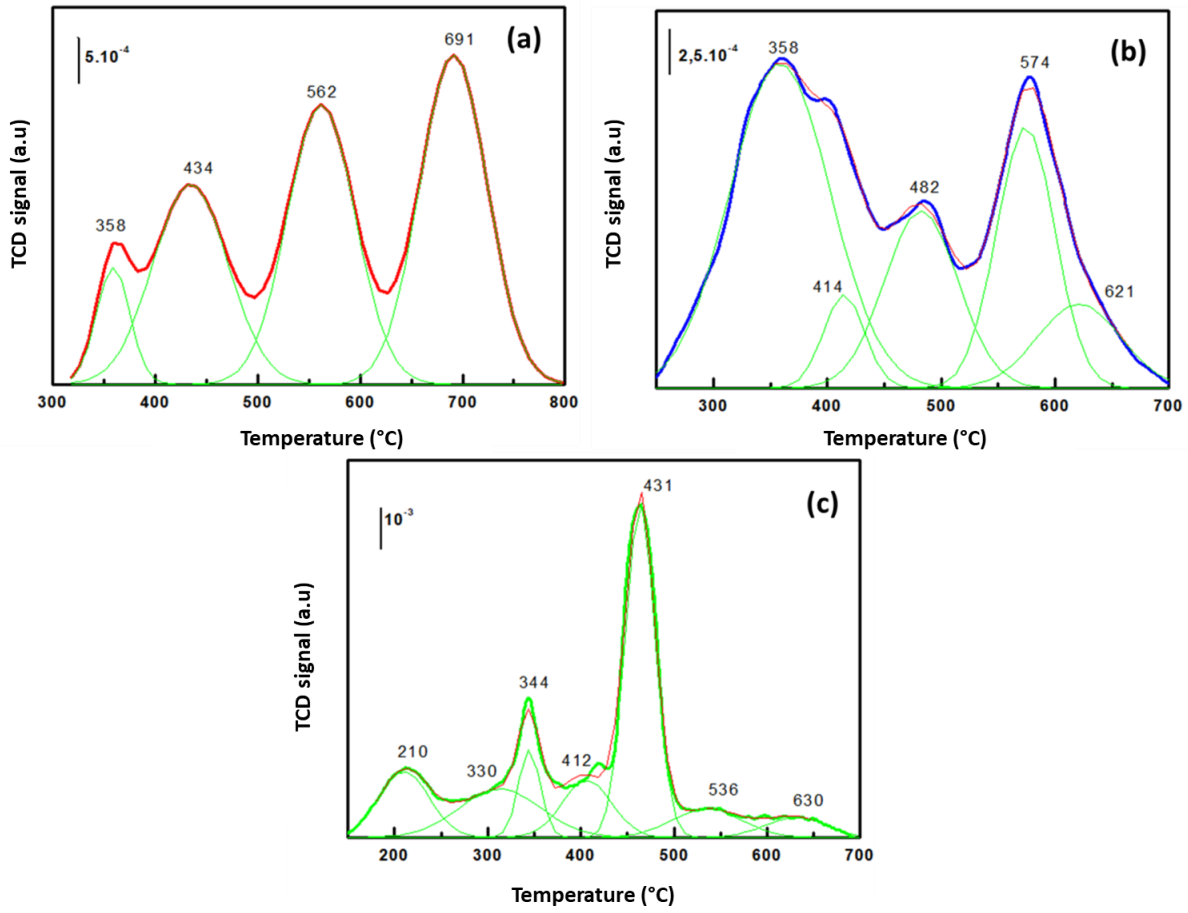

Fig. 6 H_2-TPR profiles of (a) Fe-Cu-Z-AQ, (b) Fe-Cu-Z-IM and (c) Fe-Cu-Z-SS. Pre-treatment: 30 min at 500 °C (10 °C min^{-1}) under 5%O_2/He flow (30 cm^3 min^{-1}) and then cooled under helium to 40 °C. Sample: 50 mg.

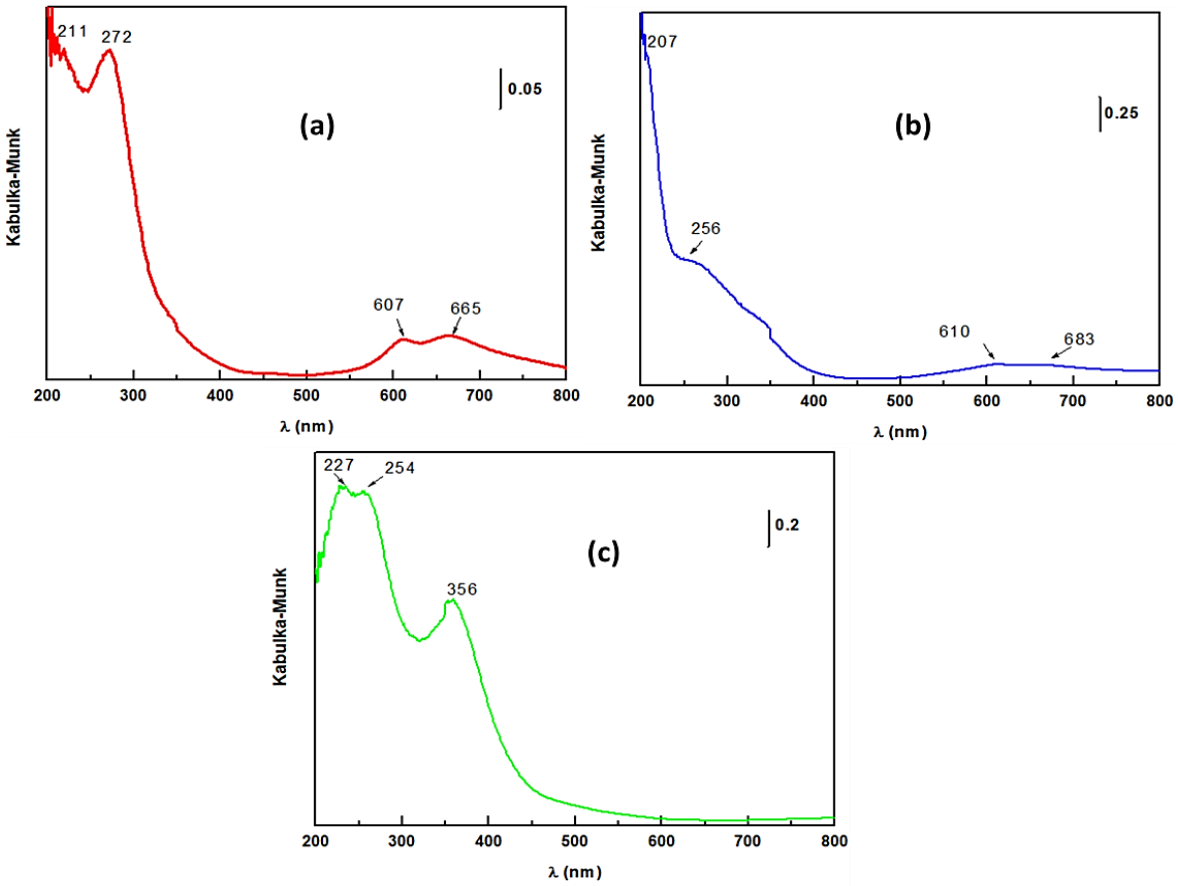

Fig. 7 DRS UV-vis spectra of fresh (a) Fe-Cu-Z-AQ, (b) Fe-Cu-Z-IM and (c) Fe-Cu-Z-SS. Temperature: room temperature. Reference material: $BaSO_4$.